Lowering plasma frequency by enhancing the effective mass of electrons: A route to deep sub-wavelength metamaterials*

Qin Gang(秦 刚)[a], Wang Jia-Fu(王甲富)[b]†, Yan Ming-Bao(闫明宝)[b], Chen Wei(陈 维)[b], Chen Hong-Ya(陈红雅)[b], and Li Yong-Feng(李勇峰)[b]

[a] College of Electronic Information Engineering, Xi'an Technological University, Xi'an 710032, China
[b] College of Science, Air Force Engineering University, Xi'an 710051, China

(Received 11 December 2012; revised manuscript received 19 January 2013)

Deep sub-wavelength metamaterials are the key to the further development of practical metamaterials with small volumes and broadband properties. We propose to reduce the electrical sizes of metamaterials down to more sub-wavelength scales by lowering the plasma frequencies of metallic wires. The theoretical model is firstly established by analyzing the plasma frequency of continuous thin wires. By introducing more inductance elements, the effective electron mass can be enhanced drastically, leading to significantly lowered plasma frequencies. Based on this theory, we demonstrate that both the electric and the magnetic plasma frequencies of metamaterials can be lowered significantly and thus the electrical sizes of metamaterials can be reduced to more sub-wavelength scales. This provides an efficient route to deep sub-wavelength metamaterials and will give rigorous impetus for the further development of practical metamaterials.

Keywords: metamaterials, deep sub-wavelength, plasma frequency, effective electron mass

PACS: 73.20.Mf, 41.20.Jb, 77.22.–d, 84.90.+a **DOI:** 10.1088/1674-1056/22/8/087302

1. Introduction

Metamaterials refer to artificial materials exhibiting unique physical properties that cannot be found in natural materials, such as negative permeability/permittivity, extremely high refractive index, zero refractive index.[1–5] In practice, metamaterials are realized by embedding sub-wavelength inclusions into a matrix.[6,7] These small inclusions are analogous to atoms and molecules in natural materials and the properties of metamaterials are dependent on the detailed configurations of these sub-wavelength inclusions. By modifying the inclusion details, the interactions between electromagnetic waves and metamaterials can be modulated to achieve diverse functional materials such as sub-wavelength imaging, metamaterial cloaks, perfect absorbers, negative reflection metasurfaces, etc.[8–13]

The fascinating properties and design freedom of metamaterials have attracted scientists from many fields, and an increasing number of metamaterial designs have been put forward.[14–18] However, most existing metamaterials are not sufficiently electrically small to be treated as "materials". As is well known, the properties of natural materials are mainly dependent on atoms or molecules which are extremely electrically small even at optical frequencies. This guarantees the validity of macroscopic description of natural materials by constitutive parameters. In analogy, to be "materials" strictly, the inclusions of metamaterials must be as electrically small as possible.[19,20] Meanwhile, from the perspective of practical applications, one of the important advantages of metamaterials is their small volume/thickness. However, since metamateials are based on resonances, their bandwidth is quite narrow. To expand the bandwidth, more inclusions must be added, which usually means the increase of the volume/thicknes. To solve this contradiction, the electrical sizes of metamaterial inclusions must be reduced, which again needs the design of deep sub-wavelength metamaterials. Hence, the design of deep sub-wavelength metamaterials has become a crucial research theme for the further development of metamaterials.

In this paper, we propose to realize deep sub-wavelength metamaterails based on enhanced effective electron mass. By introducing more inductance elements in metamaterial inclusions, the electron mass is significantly enhanced and thus the plasma frequency is reduced. A theoretical model for lowering plasma frequency of continuous thin wires is established, which lays the theoretical foundation for designing sub-wavelength metamaterials. The canonical I-shaped electric metamaterials and the short wire pair magnetic metamaterails are taken as explicit examples to demonstrate this design theory. Because of lowered electric/magnetic plasma frequencies, the electrical sizes of metamaterials are significantly reduced, which provides an efficient route to deep sub-wavelength metamaterials.

*Project supported by the National Natural Science Foundation of China (Grants Nos. 11204378 and 11274389) and the Natural Science Foundation of Shaanxi Province, China (Grant No. 2011JQ8031).

†Corresponding author. E-mail: wangjiafu1981@126.com

© 2013 Chinese Physical Society and IOP Publishing Ltd

2. Lowering the plasma frequency of metallic wires

Currently, most metamaterial inclusions are delicately-designed metallic patterns which can be treated as combinations of metallic wires. Metallic wires can be considered as the basic component of metamaterial inclusions. Hence, we start our analysis from the canonical continuous thin wires.

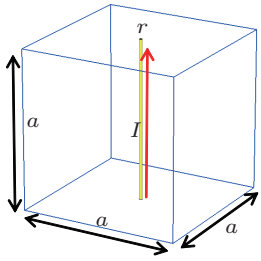


Fig. 1. (color online) A continuous thin wire in a cubic lattice.

Figure 1 gives a schematic illustration of a continuous thin wire in a cubic lattice. For such a thin wire, the plasma frequency is significantly reduced. Detailed deduction of the continuous straight thin wire plasma frequency is given in Ref. [1]. Suppose that the effective electron density of this unit cell is n_{eff} and the effective mass of electrons in the thin wire is m_{eff}. Then, the plasma frequency of this thin wire can be expressed as

$$\omega_{\text{p}} = \sqrt{\frac{n_{\text{eff}} e^2}{\varepsilon_0 m_{\text{eff}}}}. \tag{1}$$

In Eq. (1), $n_{\text{eff}} = n\pi r^2/a^2$, where n is the electron density in metal and r is the radius of the thin wire. Any restoring force acting on the electrons will have to work not only against the rest mass of the electrons, but also against self-inductance of the wire. Because of this, the effective electron mass in thin wires is greatly enhanced compared with the rest mass of electrons. For a straight wire, the effective mass of electrons is

$$\begin{aligned} m_{\text{eff}} &= \frac{\mu_0 \pi r^2 e^2 n}{2\pi} \ln\left(\frac{a}{r}\right) \\ &= e^2 \left(\pi r^2 n\right) \left[\frac{\mu_0}{2\pi} \ln\left(\frac{a}{r}\right)\right] = e^2 N_{\text{v}} L_{\text{v}}, \end{aligned} \tag{2}$$

where N_{v} and L_{v} are, respectively, the total electron number per unit length and the self-inductance per unit length. That is to say, the effective mass of electrons in metallic wires is proportional to both the electron number and the inductance per unit length. Since the effective electron density is diluted and the effective electron mass is enhanced in the continuous thin wire, the plasma frequency is drastically reduced compared with that of metallic sheets/bulky metals. In this way, the plasma frequency can be reduced even to GHz frequencies. For example, for a thin aluminum wire with a radius of 1 μm in a cubic lattice 5 mm×5 mm×5 mm, the plasma frequency can be reduced down to about 8.2 GHz.[1] The ratio between the plasma wavelength and the lattice constant is about 7.3, less than 10 (strictly speaking, the ratio between the operating wavelength and lattice constant must be greater than 10 for metamaterials).

It can be found from Eq. (2) that a straight method of lowering the plasma frequency is to make the wire thinner, which is usually used in practical metamaterial design. However, such a method is limited by the precision of practical fabrication techniques. Other ways of lowering the plasma frequencies must be adopted for very delicately thin wires. It can also be found from Eq. (2) that we can resort to enhancing the effective electron mass to further lower the plasma frequency. Figure 2 shows a typical metamaterial inclusion that can lower the plasma frequency by the introduction of meander lines.

For the continuous meander wire in Fig. 2 with the same radius and in the same lattice as a straight wire, the effective electron density is larger than that in continuous straight wire since metallic part occupies more space in the lattice. Considering additional electrons in the horizontal metallic bars, the effective electron density is

$$n'_{\text{eff}} = n_{\text{eff}} \left(1 + \frac{2lm}{a}\right), \tag{3}$$

where a is the lattice constant and m is the number of horizontal bars introduced by meander sections. It appears in Eq. (3) as if the plasma frequency would be increased since the effective electron density increases. However, we can see from Eq. (1) that the plasma frequency is dependent not only on the effective electron density but also on the effective electron mass. So we must consider what happens to the effective electron mass as well.

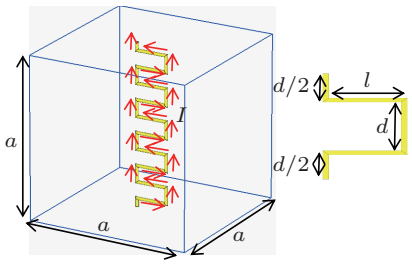


Fig. 2. (color online) A continuous meander wire in a cubic lattice. The inset shows a single meander section.

For meander wires, the inductances include both the inductance of the vertical metallic bars and the additional inductances of horizontal bars. For a periodic array of wires,

all the magnetic influxes produced by currents are confined within the unit cell and the mutual inductance actually simplifies the problem and introduces the lattice spacing as a natural cutoff.[1] Because of the modification of periodicity, the total inductance of the two horizontal bars on each meander section is

$$L_{\rm h} = l\frac{\mu_0}{\pi}\ln\left(\frac{2a}{mr}\right) = l\frac{\mu_0}{\pi}\ln\left(\frac{2d}{r}\right), \tag{4}$$

where $d = a/m$ is the distance between the two adjacent horizontal bars in a single meander section. Plus the inductance of vertical bars, the total inductance per unit length along the meander wire is

$$L = \frac{\mu_0}{2\pi}\ln\left(\frac{a}{r}\right) + \frac{ml}{a}\frac{\mu_0}{2\pi}\left[\ln\left(\frac{a}{r}\right) + \ln\left(\frac{2}{m}\right)\right]. \tag{5}$$

When $a \gg r$, equation (5) can be reduced to

$$L = \left(1+\frac{ml}{a}\right)\frac{\mu_0}{2\pi}\ln\left(\frac{a}{r}\right) = \left(1+\frac{ml}{a}\right)L_{\rm v}. \tag{6}$$

The total electron number per unit length along the meander wire is

$$N = \frac{(a+ml)\pi r^2 n}{a} = \left(1+\frac{ml}{a}\right)N_{\rm v}. \tag{7}$$

Substitute Eqs. (6) and (7) into Eq. (2), then we will have the effective electron mass in meander wires as

$$m'_{\rm eff} = e^2 NL = e^2 N_{\rm v} L_{\rm v}\left(1+\frac{ml}{a}\right)^2 = m_{\rm eff}\left(1+\frac{ml}{a}\right)^2. \tag{8}$$

Substituting Eqs. (3) and (8) into Eq. (1), we finally obtain the plasma frequency of meander wires as

$$\omega'_{\rm p} = \sqrt{\frac{n'_{\rm eff}e^2}{\varepsilon_0 m'_{\rm eff}}} = \sqrt{\frac{n_{\rm eff}(1+ml/a)e^2}{\varepsilon_0 m_{\rm eff}(1+ml/a)^2}} = \frac{\omega_{\rm p}}{\sqrt{1+ml/a}}. \tag{9}$$

We can find from Eq. (8) that although the effective electron density is increased, the plasma frequency of meander wires is nevertheless reduced since the effective electron mass is enhanced more drastically. Moreover, under a given lattice constant a, we can lower the plasma frequency by increasing the meander number m or the meander length l in a unit cell. For example, for straight aluminum wires with $r = 1$ μm and $a = 5$ mm, the plasma frequency is about 8.2 GHz; while for meander aluminum wires with $m = 4$ and $l = 4.5$, the plasma frequency is reduced to about 3.8 GHz, without scaling up the lattice size. In this way, meander wires are more sub-wavelength than straight ones, which provides an efficient route to deep sub-wavelength metamaterials. Equation (9) can also be rewritten as

$$\omega'_{\rm p} = \frac{\omega_{\rm p}}{\sqrt{1+l/d}}.$$

That is, the ratio between plasma frequencies of straight and meander wires are only dependent on the ratio between the horizontal bar length and the distance between adjacent horizontal bars.

To verify the above theoretical analysis, numerical simulations are carried out for continuous wire structures in practical metamaterial design using the frequency domain solver of CST Microwave Studio. In practical fabrication techniques such as lithography and silk-screen printing, metallic structures are usually patterned on supporting substrates. Figure 3(a) illustrates the continuous thin wire unit cell typically used in the design of left-handed metamaterials. A metallic strip (0.02-mm thick) is etched on one side of a 1-mm thick FR4 substrate ($\varepsilon_{\rm r} = 4.3$). The lattice constant is $a = 5$ mm. The metallic strip width is $w = 0.2$ mm and thus the effective radius is $r_{\rm eff} \approx w/4 = 0.05$ mm[21] for $w \ll l$. Figure 3(b) shows the corresponding meander wire with $m = 4$ horizontal bars. The length of the horizontal bars is 3.8 mm. Substituting these values into Eq. (9), then we will obtain

$$\frac{\omega'_{\rm p}}{\omega_{\rm p}} = \frac{1}{\sqrt{1+ml/a}} = \frac{1}{\sqrt{1+4\times 3.8/5}} \approx 0.5.$$

The computed plasma frequencies of the straight and meander wires are 10.68 GHz and 5.82 GHz, respectively. The computed ratio between plasma frequencies of meander and straight wires is thus about 0.54, in good agreement with that predicted using Eq. (9).

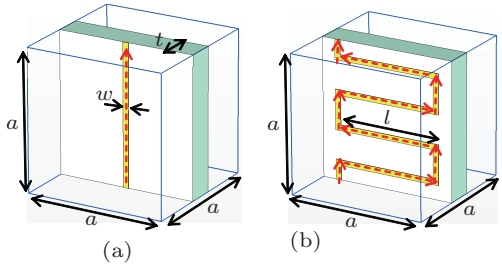


Fig. 3. (color online) Schematic illustrations of a continuous straight wire and meander wire in cubic lattices: (a) the continuous straight wire unit cell; (b) the continuous meander wire unit cell.

3. Reducing the electrical sizes of electric metamaterials

For discontinuous resonant metallic structures, the plasma frequency can also be lowered by introducing meanders since the additional meander bars provide additional inductances to enhance the effective electron mass. In addition to continuous thin wires, the discontinuous I-shaped electric metamaterial is also a good candidate for realizing broadband negative effective permittivity.[18] The effective permittivity of such electric metamaterials is in the form as[3]

$$\varepsilon_{\rm r}(\omega) = 1 - \frac{\omega_{\rm pe}^2 - \omega_{\rm oe}^2}{\omega^2 - \omega_{\rm oe}^2 + {\rm i}\gamma\omega},$$

where ω_{pe} and ω_{oe} are the electric plasma frequency and electric resonance frequency, respectively, and γ is the dissipation factor. In lossless case $\gamma = 0$, when $\omega = \omega_{pe}$, $\varepsilon_r(\omega) = 0$; when $\omega = \omega_{oe}$, $\varepsilon_r(\omega) \to \infty$.

The electric plasma frequency of I-shaped electric metamaterial can also be lowered by introducing meander bars. For discontinuous metallic structures, the sizes in all the directions are shorter than the lattice constant, so Eq. (9) should be modified as

$$\frac{\omega'_{pe}}{\omega_{pe}} = \frac{1}{\sqrt{1+ml/l_1}}. \tag{10}$$

To verify our analysis, we carry out numerical simulation for a typical I-shaped electric metamaterial. Figure 4(a) shows the unit cell of this electric metamaterial. The I-shaped metallic pattern is etched on one side of a 1-mm thick FR4 substrate ($\varepsilon_r = 4.3$). The strip width is $w = 0.2$ mm and the lengths of the metallic strips are $l_1 = l_2 = 4$ mm. The lattice constant is $a = 5$ mm. Figure 4(b) shows the corresponding meander version of I-shaped electric metamaterial. Instead of a straight central bar, 3 more horizontal bars ($m = 3$) each with a length of $l = 4$ mm are introduced in the meander version. Using Eq. (10), it can be predicted that $\omega'_{pe}/\omega_{pe} = 1/\sqrt{1+3\times 4/4} = 0.5$.

Figures 5(a) and 5(b) give, respectively, the simulated transmission spectra for the straight I-shaped and the meander I-shaped electric metamaterials. Comparing Fig. 5(a) with Fig. 5(b), we can find that the transmission dip is lowered from 10.2 GHz to about 5.0 GHz under the unchanged lattice constant $a = 5$ mm. Figures 5(c) and 5(d) give the retrieved effective permittivity values of the straight and the meander I-shaped electric metamaterials, respectively. As shown in Figs. 5(c) and 5(d), the electric plasma frequency is lowered from 14.0 GHz to 7.0 GHz, in excellent agreement with that predicted by Eq. (10). Moreover, the electric resonance frequency is also lowered from 8.4 GHz to 4.8 GHz. That is to say, both the electric resonance frequency and electric plasma frequency are lowered significantly for the meander electric metamaterial through the introduction of meanders. Thus, in the operating band, the electrical sizes of electric metamaterials can be reduced significantly.

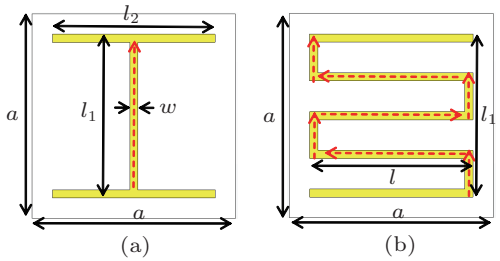


Fig. 4. (color online) Unit cells of the straight and meander I-shaped electric metamaterials: (a) straight I-shaped unit cell; (b) meander I-shaped unit cell.

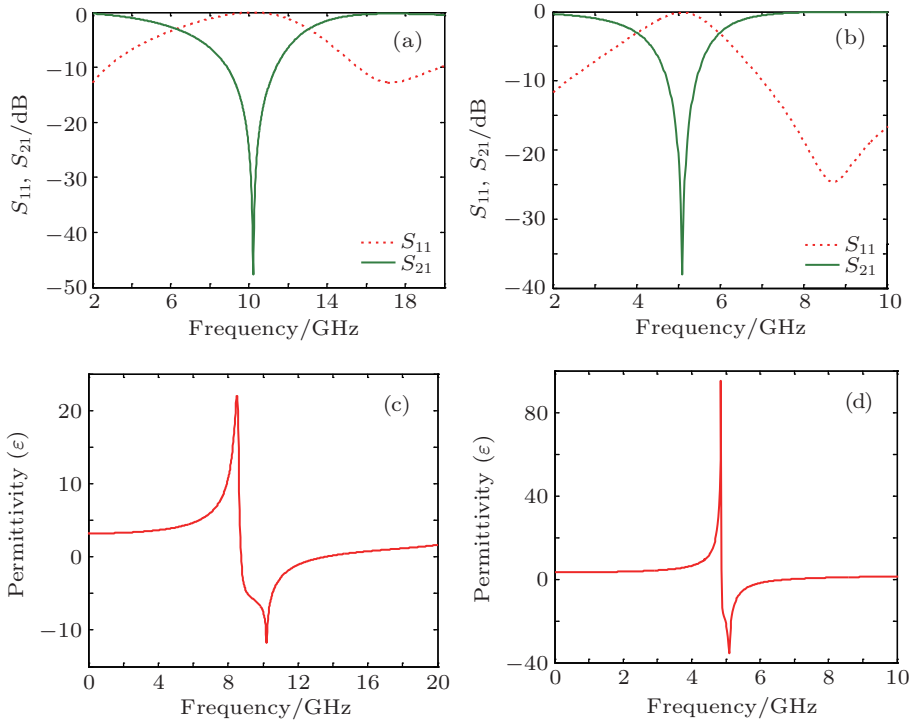


Fig. 5. (color online) Transmission spectra and effective permittivity for the electric metamaterials: (a) S_{11} and S_{21} parameters of the straight I-shaped electric metamaterial; (b) S_{11} and S_{21} parameters of the meander I-shaped electric metamaterial; (c) effective permittivity of straight I-shaped electric metamaterial; (d) effective permittivity of meander I-shaped electric metamaterial.

4. Reducing the electrical sizes of magnetic metamaterials

Magnetic metamaterials realize negative effective permeability values by their magnetic resonances in response to external magnetic fields. The effective permeability is in the form as[3]

$$\mu_{\rm r}(\omega) = 1 - \frac{\omega_{\rm pm}^2 - \omega_{\rm om}^2}{\omega^2 - \omega_{\rm om}^2 + {\rm i}\gamma\omega},$$

where $\omega_{\rm pm}$ and $\omega_{\rm om}$ are the magnetic plasma frequency and magnetic resonance frequency, respectively, and γ is the dissipation factor. In lossless case $\gamma = 0$, when $\omega = \omega_{\rm pm}$, $\mu_{\rm r}(\omega) = 0$; when $\omega = \omega_{\rm om}$, $\mu_{\rm r}(\omega) \to \infty$.

To achieve strong magnetic resonances, most magnetic metamaterials, like split-ring resonators,[2] require incident EM waves to be in parallel with the substrate, which brings troubles in fabricating and applying these magnetic metamaterials. Fortunately, there are also magnetic metamaterials that allow normal incidence.[13] A typical normal-incidence magnetic metamaterial is the short wire pair structure[18] as shown in Fig. 6(a). The unit cell is composed of two identical metallic short wires etched on both sides of a dielectric substrate. Two fundamental modes exist for such a structure in response to external EM waves: anti-symmetric mode with anti-parallel surface currents and symmetric mode with parallel surface currents. The short wire pair magnetic metamaterial operates just under the first mode, anti-symmetric mode. Under this mode, anti-parallel surface currents on the short wire pair, plus the displacement current in between the two short wires, form an effective current loop which is equivalent to a magnetic dipole. Strong diamagnetic response of this equivalent magnetic dipole will bring the effective permeability down in the resonance regime. However, such a magnetic metamaterial is only sub-wavelength along the normal of the substrate, usually about half wavelength along the wire direction. To act as a magnetic metamaterial strictly, the planar sizes of the short wire pair unit cell must be reduced.

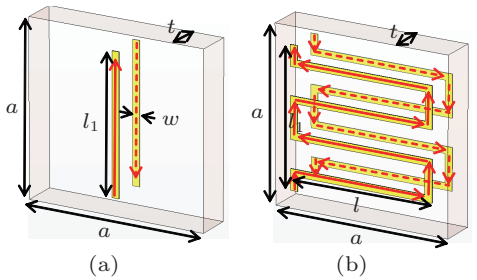


Fig. 6. (color online) Unit cells of short wire pair magnetic metamaterials and the corresponding meander-modified version: (a) the short wire pair; (b) the meander-modified short wire pair.

Figure 6(b) shows the corresponding meander-modified version of the short wire pair magnetic metamaterial. Two identical meander wires with m (in Fig. 6(b), as an example, $m = 4$) additional horizontal bars are etched on both sides of a dielectric substrate. The effective electron density is

$$n'_{\rm eff} = \left(\frac{2l_1 + 2lm}{2l_1}\right) n_{\rm eff} = \left(1 + \frac{lm}{l_1}\right) n_{\rm eff}, \tag{11}$$

where $n_{\rm eff}$ denotes the effective electron density of the straight short wire pair. Then, the total electron number per unit length is

$$N = \left(1 + \frac{ml}{l_1}\right) N_{\rm v}, \tag{12}$$

where $N_{\rm v}$ denotes the total electron number per unit length for the straight short wire pair.

To obtain the effective electron mass, we must firstly analyze the inductance of the meander short wire pair. The inductance includes mainly three parts: inductance of the vertical connecting bars $L_{\rm v}$, inductance of horizontal bars on the same side $L_{\rm h1}$, and mutual inductance of horizontal bar on both sides $L_{\rm h2}$. From the inductance formula of two parallel wires in electromagnetic theories,[22] the three kinds of inductances are, respectively,

$$L_{\rm v} = l_1 \frac{\mu_0}{\pi} \ln\left(\frac{a}{r_{\rm eff}}\right), \tag{13}$$

$$L_{\rm h1} = 2ml \frac{\mu_0}{\pi} \ln\left(\frac{a}{r_{\rm eff}}\right), \tag{14}$$

$$L_{\rm h2} = m^2 l \frac{\mu_0}{2\pi} \ln\left(\frac{a}{r_{\rm eff}}\right), \tag{15}$$

where t and $r_{\rm eff}$ are the thickness of the substrate and the effective radius of the metallic strip. The total inductance per unit length is thus

$$L = \frac{L_{\rm v} + L_{\rm h1} + L_{\rm h2}}{a} = \frac{l_1}{a}\frac{\mu_0}{\pi} \ln\left(\frac{a}{r_{\rm eff}}\right) + \frac{2ml}{a}\frac{\mu_0}{\pi} \ln\left(\frac{a}{r_{\rm eff}}\right) + \frac{m^2 l}{a}\frac{\mu_0}{2\pi} \ln\left(\frac{a}{r_{\rm eff}}\right). \tag{16}$$

Equation (16) can be reduced to

$$L = \left[1 + \frac{(2m + m^2/2)l}{l_1}\right] L_{\rm v}. \tag{17}$$

Substituting Eqs. (17) and (12) into Eq. (2), then we will obtain the effective electron mass as

$$m'_{\rm eff} = e^2 NL = \left(1 + \frac{ml}{l_1}\right)\left[1 + \frac{(2m + m^2/2)l}{l_1}\right] m_{\rm eff}. \tag{18}$$

Substituting Eqs. (18) and (11) into Eq. (1), we finally obtain the magnetic plasma frequency as

$$\omega'_{\rm pm} = \sqrt{\frac{n'_{\rm eff} e^2}{\varepsilon_0 m'_{\rm eff}}} = \frac{\omega_{\rm pm}}{\sqrt{1 + (2m + m^2/2)l/l_1}}, \tag{19}$$

where $\omega_{\rm pm}$ denotes the magnetic plasma frequency of the straight short wire pair.

To verify the above theoretical analysis, numerical simulations are carried out for the straight and meander short wire

pair. For the straight short wire pair, the geometrical parameters are as follows: $a = 5$ mm, $l_1 = 4$ mm, $w = 0.2$ mm. FR4 substrate with a thickness $t = 1$ mm and dielectric constant $\varepsilon_r = 4.3$ is used. For the meander short wire pair, $m = 4$ horizontal bars are introduced and the geometrical parameters are as follows: $a = 5$ mm, $l_1 = 4$ mm, $t = 1$ mm, $w = 0.2$ mm, $l = 4$ mm. Using Eq. (19), it can be predicted that the ratio between the magnetic plasma frequencies of straight and meander short wire pairs is

$$\frac{\omega'_{\rm pm}}{\omega_{\rm pm}} = \frac{1}{\sqrt{1+(2m+m^2/2)l/l_1}} \approx 0.24.$$

Figures 7(a) and 7(b) show the simulated transmission spectra of the straight and meander short wire pair magnetic metamaterials, respectively. There are two transmission dips in Figs. 7(a) and 7(b), corresponding to the anti-symmetric and symmetric modes, respectively. The anti-symmetric mode is drastically reduced from about 21.0 GHz to 5.0 GHz. The ratio between the magnetic plasma frequencies of straight and meander short wire pairs is about 0.238, highly consistent with the predicted result using Eq. (19). Hence, by the introduction of meander lines, the size of short wire pair magnetic metamaterial is reduced from about $\lambda/3$ to less than $\lambda/12$, strictly sub-wavelength in all the directions of the lattice. Note that the electric plasma frequency under symmetric mode is also reduced to about a quarter that of the straight short wire

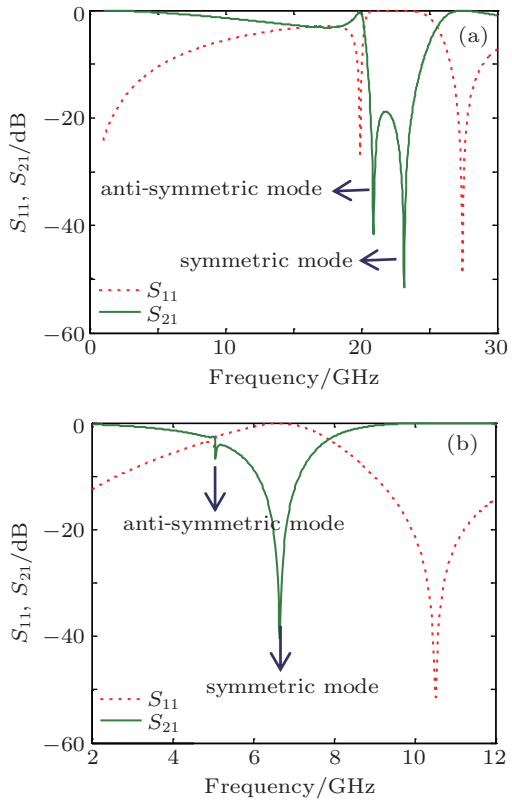


Fig. 7. (color online) Transmission spectra of the straight and meander short wire pair metamaterials: (a) transmission spectra of straight short wire pair; (b) transmission spectra of meander short wire pair.

pair. Since the meander short wire pair metamaterial is strictly sub-wavelength, it can be described by the effective medium theory. Figures 8(a) and 8(b) present the effective permeability and permittivity of the meander short wire pair metamaterial. As shown in Fig. 8, the effective permeability is negative in a frequency range of 5.0 GHz–5.1 GHz ($f_{\rm om} = 5.0$ GHz, $f_{\rm pm} = 5.1$ GHz) under the anti-symmetric mode, which is just the operating band of the short wire pair magnetic metamaterial. Moreover, in a frequency range of 6.15 GHz–8.5 GHz ($f_{\rm oe} = 6.15$ GHz, $f_{\rm pe} = 8.5$ GHz), the meander short wire pair can also act as an electric metamaterial with negative effective permittivity.

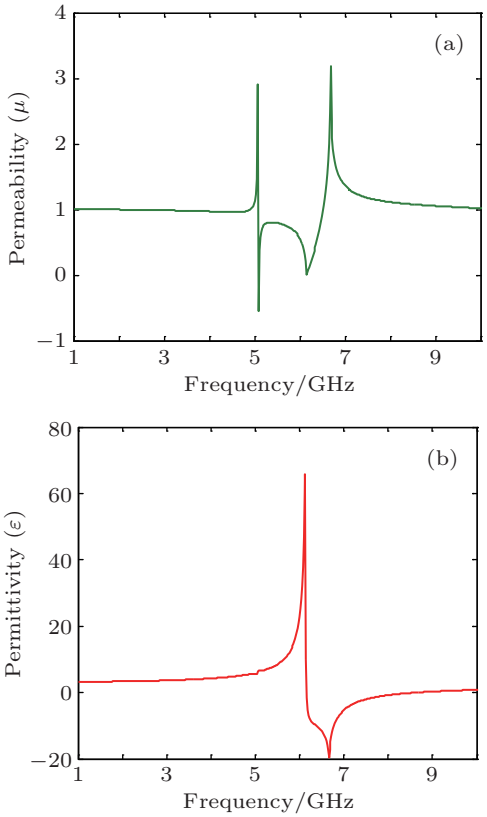


Fig. 8. (color online) Effective permeability and permittivity of the meander short wire pair metamaterial: (a) effective permeability; (b) effective permittivity.

5. Conclusions

In this paper, we propose and demonstrate the theory of realizing deep sub-wavelength metamaterials by lowering the plasma frequencies of metamaterial inclusions. By adding more inductance elements, the effective electron mass is drastically enhanced. In this way, plasma frequencies of both the electric and magnetic metamaterials can be significantly lowered and thus the electrical sizes of metamaterial inclusions are reduced to deep sub-wavelength scales. Because more metallic parts are adopted within the small volume, more absorption losses are introduced. Nevertheless, the theory provides an efficient route to deep sub-wavelength metamaterials and

thus will give vigorous impetus for the further development of ultra-thin, broadband metamaterials.

References

[1] Pendry J B, Holden A J, Stewart W J and Youngs I 1996 *Phys. Rev. Lett.* **76** 4773

[2] Pendry J B, Holden A J, Robbins D J and Stewart W J 1999 *IEEE Trans. Microwave Theory Tech.* **47** 2075

[3] Shelby R A, Smith D R and Schultz S 2001 *Science* **292** 77

[4] Choi M, Lee S H, Kim Y, Kang S B, Shin J, Kwak M H, Kang K Y, Lee Y H, Park N and Min B 2011 *Nature* **470** 369

[5] Huang X Q, Lai Y, Hang Z H, Zheng H H and Chan C T 2011 *Nat. Mater.* **10** 582

[6] Holloway C L, Kuester E F, Baker-Jarvis J and Kabos P 2003 *IEEE Trans. Antenn. Propag.* **51** 2596

[7] Wang J F, Qu S B, Yang Y M, Ma H, Wu X and Xu Z 2009 *Appl. Phys. Lett.* **95** 014105

[8] Schurig D, Mock J J, Justice B J, Cummer S A, Pendry J B, Starr A F and Smith D R 2006 *Science* **314** 977

[9] Landy N I, Sajuyigbe S, Mock J J, Smith D R and Padilla W J 2008 *Phys. Rev. Lett.* **100** 207402

[10] Hao J M, Yuan Y, Ran L X, Jiang T, Kong J A, Chan C T and Zhou L 2007 *Phys. Rev. Lett.* **99** 063908

[11] Sun S L, He Q, Xiao S Y, Xu Q, Li X and Zhou L 2012 *Nat. Mater.* **11** 426

[12] Ma H, Qu S B, Xu Z and Wang J F 2009 *Opt. Lett.* **34** 127

[13] Liu Z W, Lee H, Xiong Y, Sun C and Zhang X 2007 *Science* **315** 1686

[14] Wang J F, Qu S B, Xu Z, Ma H, Xia S, Yang Y M, Wu X, Wang Q and Chen C H 2010 *Phys. Rev. E* **81** 036601

[15] Chen H S, Ran L X, Huangfu J T, Zhang X M, Chen K S, Grzegorczyk T M and Kong J A 2004 *Phys. Rev. E* **70** 057605

[16] Tang W X, Zhao H, Zhou X Y, Chin J Y and Cui T J 2008 *Prog. Electromag. Res. B* **8** 103

[17] Chen C H, Qu S B, Xu Z, Wang J F, Ma H and Zhou H 2011 *Acta Phys. Sin.* **60** 024101 (in Chinese)

[18] Zhou J F, Zhang L, Tuttle G, Koschny T and Soukoulis C M 2006 *Phys. Rev. B* **73** 041101

[19] Koschny T, Kafesaki M, Economou E N and Soukoulis C M 2004 *Phys. Rev. Lett.* **93** 107402

[20] Simovski C R and Tretyakov S A 2007 *Phys. Rev. B* **75** 195111

[21] Lo Y T and Lee S W 1988 *Antenna Handbook: Theory, Applications, and Design* (New York: Van Nostrand Reinold Co.)

[22] Xie C F and Rao K J 2006 *Electromagnetic Fields and Electromagnetic Waves* (Beijing: Higher Education Press) (in Chinese)